Moving between dimensions in electromagnetic inversions

Seogi Kang, Rowan Cockett, Lindsey J. Heagy, & Douglas W. Oldenburg, Geophysical Inversion Facility, University of British Columbia*

SUMMARY

Electromagnetic (EM) methods are used to characterize the electrical conductivity distribution of the earth. EM geophysical surveys are increasingly being simulated and inverted in 3D, due in part to computational advances. However, the availability of computational resources does not invalidate the use of lower dimensional formulations and methods, which can be useful depending on the geological complexity as well as the survey geometry. Due to their computational speed, simulations in 1D or 2D can also be used to quickly gain geologic insight. For example, this insight can be used in an EM inversion starting with a 1D inversion, then building higher dimensionality into the model progressively. As such, we require a set of tools that allow a geophysicists to easily explore various model dimensionalities, such as 1D, 2D, and 3D, in the EM inversion. In this study, we suggest a mapping methodology that transforms the inversion model to a physical property for use in the forward simulations. Using this general methodology, we apply an EM inversion to a suite of models in one, two, and three dimensions, and suggest the importance of choosing an appropriate model space based on the goal of the EM inversion.

INTRODUCTION

Electromagnetic (EM) fields and fluxes can be used to excite the earth, and in a geophysical survey, we measure and interpret the resulting signals. These signals are sensitive to the conductivity distribution of the earth. By numerically solving Maxwell's equations, we can compute the forward response for a system with a known conductivity distribution. To conduct a forward simulation for a 3D conductivity distribution, we require the property to be discretized numerically, and we typically employ a voxel-based mesh to discretize the earth. Once we have a mechanism to simulate EM fields and fluxes, we can consider approaching the inverse problem. The aim of an EM inversion is to recover a model that is consistent with the measured EM data and prior knowledge of the geologic setting.

Three dimensional EM inversion techniques using gradient-based optimization have been actively developed and applied for various survey types and geologic settings (Oldenburg et al. (2013); Gribenko and Zhdanov (2007); Chung et al. (2014)). A gradient based inversion approach requires defining an objective function that will be minimized in the optimization. Equally important, yet often overlooked, is the definition of the model over which we minimize. Our focus in this paper is the construction of this inversion model in a flexible framework.

In practice, a log-conductivity model with the same dimensionality as the forward modelling mesh is often chosen to be the inverse model, m. To construct the conductivity distribution from m requires a mapping to return to physical parameter space:

$$\sigma(m) = \mathscr{M}[m], \tag{1}$$

which takes us from the space of the inverse model m to physical property space. In the case of a log-conductivity model, the mapping is simply $\mathscr{M}[m] = \exp(m)$. We can also consider constructing mappings in which the inverse model m and the physical property distribution σ have differing dimensionalities. We will motivate this discussion using a 3D conductivity model of a seawater intrusion, shown in Figure 1. Although the physical property model must be described in 3D, the inversion model may have lower spatial dimensionality, as shown conceptually in Figure 1. A mapping, $\mathscr{M}[\cdot]$, is necessary to transform between the inversion model and the physical property distribution. Moving between the spatial dimensionalities of our chosen model (e.g. 1D to 3D or 2D to 3D) is possible through the use of this mapping function. Alternatively, we can consider parametric models, in which the mapping takes a description of a geometric shape with a small number of parameters, such as a sphere or ellipsoid, and returns the 3D physical property distribution (cf. Pidlisecky et al. (2011); McMillan et al. (2014)) or parameterizations of the inversion model space (cf. Heagy et al. (2014)). The numerical implementations shown in this abstract are conducted using SIMPEGEM which is part of a software ecosystem for Simulation and Parameter Estimation in Geophysics (Cockett et al. (2015)). SIMPEGEM provides forward modeling and geophysical inversion of EM methods in both frequency and time domain (Kang et al. (2015)).

In this study, we select a seawater intrusion model and use a ground loop time domain EM (TDEM) survey to demonstrate the diversity of model spaces that we can choose for the EM inversion. A 3D forward simulation is performed to obtain synthetic data, which we treat as our observed data for the inversion. We approach the inverse problem in a progressive manner by starting with stitched 1D inversions, moving to a 2D inversion for a line of data, and finally performing a 3D inversion to obtain a 3D physical property model describing the seawater intrusion.

METHODOLOGY

In the EM inversion, we attempt to recover a model which explains measured response and is consistent with our prior knowledge. The EM response is governed by Maxwell's equations and depends upon the electrical conductivity (σ), which is a physical property distributed in 3D space: $\sigma = \sigma(x,y,z)$. We excite the earth using a time-varying current, $\vec{j}_s$, and measure EM response at receiver locations. By discretizing Maxwell's equations, we can numerically compute the forward response. This operation can be succinctly written as

$$d^{pred} = F[\sigma], \tag{2}$$

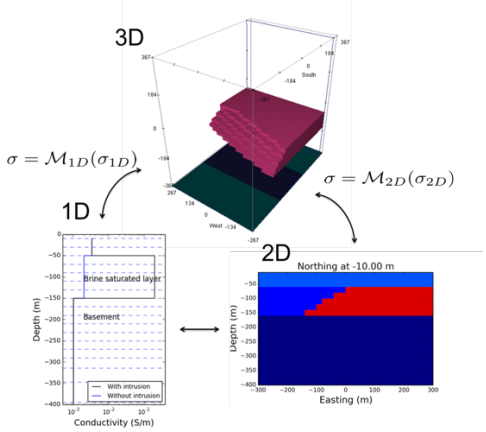

Figure 1: Conceptual diagram of moving between 1D, 2D, and 3D models.

where $F[\cdot]$ is the Maxwell operator and d^{pred} is the computed EM response at the receiver locations. A major goal of the EM survey is to recover the conductivity distribution. To achieve this goal, we use geophysical inverse theory and gradient-based optimization. We minimize an objective function ($\phi(m)$):

$$\phi(m) = \phi_d(\sigma(m)) + \beta\phi_m(m), \tag{3}$$

where m is the inversion model, ϕ_d is the data misfit, ϕ_m is the model regularization term, and β is a trade-off parameter between ϕ_d and ϕ_m. For further discussion on the selection of ϕ_d, ϕ_m and β see, for example, Oldenburg and Li (2005). To evaluate the data misfit term, we must perform a forward simulation, which requires having the physical property σ defined on our forward modelling mesh. Using the map defined in equation 1, we can transform the inversion model, m to conductivity σ. Although this map can be an identity, the general case allows us to explore various parameterizations of our model space, with minimal changes to an inversion implementation.

The core of the gradient-based optimization is the sensitivity function (the derivative of the forward simulation with respect to the inversion model):

$$J = \frac{\partial F[\sigma]}{\partial m} = \frac{\partial d^{pred}}{\partial \sigma}\frac{\partial \sigma}{\partial m}. \tag{4}$$

Assuming that we know how to compute $\frac{\partial F[\sigma]}{\partial \sigma}$, we can proceed to compute the sensitivity so long as we know the derivative of the mapping function ($\frac{\partial \sigma}{\partial m} = \frac{\partial \mathcal{M}(m)}{\partial m}$). This mapping is not restricted to being a single function, but may be a composition of multiple functions, and the computation of the derivative can be defined using the chain-rule. For example, often in EM inversions, we use logarithmic conductivity as our model, and we do not include air cells in the definition of our inversion model. In this case, our mapping can be expressed as a combination of the exponential ($\mathcal{M}_{exp}[\cdot]$) and an 'surjection map' ($\mathcal{M}_{surj}[\cdot]$):

$$\sigma = \mathcal{M}_{exp}[\mathcal{M}_{surj}[m]]. \tag{5}$$

The output of the combined mapping function should be σ defined everywhere in the forward modelling domain. We break apart the combined mapping function above into two parts and define the number of cells in the domain and the active region as n_C and n_{active}, respectively. The first part is the surjection map: this takes the input, in this case a model, m, that is defined in the active region, and injects the values in to the entire domain which includes the inactive model. The output of this mapping function as it is used in equation 5 is $log(\sigma)$ in the entire forward modelling domain. Our forward modelling requires σ, so we use an exponential map to obtain 3D conductivity as

$$\sigma = \mathcal{M}_{exp}(log(\sigma)) = e^{log(\sigma)}. \tag{6}$$

Note that this is done point-wise, that is, we use the vector notation $(e^{log(\sigma)})_i = e^{log(\sigma_i)}$. The derivative of the combined mapping function can be expressed as

$$\frac{\partial \mathcal{M}_{exp}[\mathcal{M}_{surj}[m]]}{\partial m} = \frac{\partial \mathcal{M}_{exp}[\mathcal{M}_{surj}[m]]}{\partial \mathcal{M}_{surj}[m]}\frac{\partial \mathcal{M}_{surj}[m]}{\partial m}$$

where $diag(\cdot)$ indicates a diagonal matrix.

Similar to the exponential mapping, we can create a vertical 1D map ($\mathcal{M}_{1D}[\cdot]$) that repeats a model vector vertically everywhere in the 3D domain. The combined mapping shown in equation (5), can be modified as

$$\sigma = \mathcal{M}_{exp}[\mathcal{M}_{1D}[\mathcal{M}_{surj}[m]]]. \tag{7}$$

This mapping procedure is graphically illustrated in Figure 2. Our model is in the active domain (i.e. the subsurface) and contains logarithmic conductivity values, (Figure 2a). With the surjection map, we fill in the additional model cells for modelling the air ($log(\sigma_{air})$), these cells are necessary for our 1D map. The last two steps of our mapping are shown in Figure 2c, where the 1D logarithmic conductivity is extended in the x and y directions filling the entire domain, and finally the exponential map brings us to conductivity values. Application to a 2D map is identical to equation 7 except that our inversion model is in two dimensions and we must pick a plane of symmetry. For example, we can choose logarithmic conductivity of the subsurface defined on x-z plane as our model. This often called a 2.5D inversion as the model is in 2D although the forward simulation is performed in 3D.

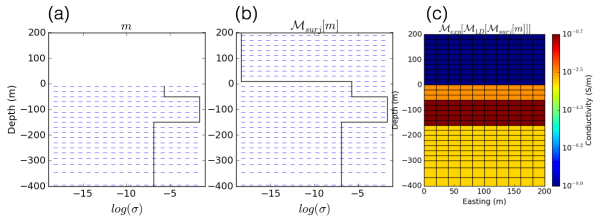

Figure 2: A graphical illustration of the combined map shown in equation (7), which transforms (a) 1D logarithmic conductivity values in the subsurface, to (b) a vertical 1D model to (c) a 3D conductivity distribution through a vertical 1D map and an exponential.

SEAWATER INTRUSION EXAMPLE

In some coastal area, seawater intrusion is a serious problem due to the resulting contamination of groundwater (Figure 3).

Moving between dimensions in EM inversions

The location and distribution of the seawater intrusion is a key piece of information to any management decisions taken to assess or address the threat of seawater intrusion. Ground loop EM surveys have been used to detect intruded seawater, because seawater is highly conductive (Mills et al. (1988)). Figure 3 shows a typical ground loop TEM survey geometry and a hydrological model of the coastal area. By putting time-varying current through the transmitter loop, we excite the earth. The 3D conductivity model shown in Figure 4 shows the true distribution of the seawater intrusion. Geophysics can be used as a tool to locate the possible region where we have serious seawater intrusion. As such, recovering the conductivity distribution, which has high correlation with the seawater intrusion is a principal task. More specifically, the interface between freshwater and seawater is crucial information.

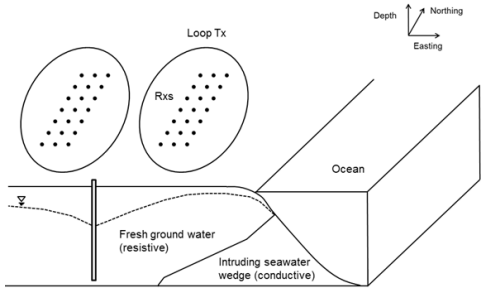

Figure 3: Conceptual diagram of seawater intrusion and geometry of ground loop EM survey.

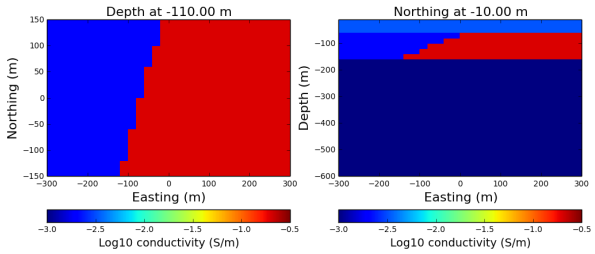

Figure 4: Plan and section views of 3D conductivity model for seawater intrusion.

Ground loop TDEM survey set-up

To simulate measured EM data collected over the intruded seawater, we design a ground loop EM survey using the geometry shown in Figure 5. The survey consists of two circular loops, each with a radius of 250 m. Receivers, which measure the vertical component of the magnetic flux density (b_z), are located inside of each transmitter, and the time-range over which we measure this response is 0.1-10 ms. The forward responses of this TDEM survey are computed using SIMPEGEM. The number of cells used in 3D forward calculation for the synthetic data is 54×44×54, and the smallest cell size is 30 m×20 m×30 m.

1D inversion

Typically for a ground loop EM survey, we only measure one or two profile lines of the data in the loop (Mills et al. (1988)).

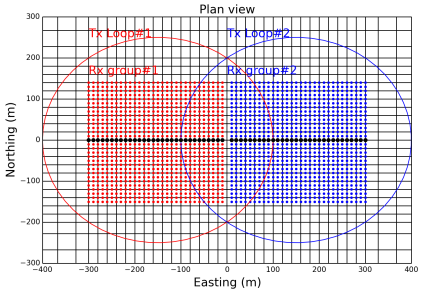

Figure 5: Ground loop EM survey geometry. Blue and red color indicate the two corresponding Tx and Rx pairs. Black dots show a line profile data used for 1D and 2D inversion.

To interpret the data, 1D EM inversions, which assume a layered-earth structure are often used. Here, we employ a separate 1D inversion for each sounding. The recovered 1D conductivity models for each sounding are then stitched together to make an interpolated 2D section.

For the 1D inversion, conventionally, pseudo-analytic solutions of the layered-earth medium is used, which requires evaluation of infinite integration **??**. Instead, we use a cylindrical mesh with coordinates of r, θ, and z, and exploit the azimuthal symmetry of the system (i.e. properties are constant in θ), which does not require infinite integration, but needs solving of a 2D partial differential equation using finite volume. Our inversion model in this case is the logarithmic conductivity with vertical 1D cells in the subsurface. The number of cells in 2D mesh is 45×70, whereas that of 1D inversion subsurface model is only 35. Here we require a mapping function that takes the inversion model and transfers it to conductivity on the cylindrical mesh. Using the mapping shown in equation (7), we can obtain the conductivity on the 2D cylindrical mesh. Consistent with a typical field configuration, we only used a profile line in two loop sources for the 1D inversion, which are shown as black dots in Figure 5. The recovered 1D stitched inversion model, on the left panel of Figure 6, shows reasonable layering on the east-side. However, on the west-side, there are artifacts that are likely due to 3D effects. That is, the inversion model dimensionality is inconsistent with the complexity required to explain the data. These results are consistent with the equivalent approach of a layered earth inversion.

2D inversion

To consider multi-dimensional effect from intruded seawater, we increase the dimensionality in our inversion to two dimensions. This increase in dimensionality breaks our assumption of cylindrical symmetry, so we must switch our forward modeling to a 3D tensor product mesh. For this case, we assume that 3D conductivity is invariant in the y-direction. Using the mapping function shown in equation (7), we obtain 3D conductivity from 2D logarithmic conductivity model in the subsurface. The number of cells in 3D mesh is 54×40×54, whereas the 2D model has 54×27 cells. The right panel of Figure 6 shows the recovered conductivity model from the 2D inversion. This shows better horizontal resolution than the 1D

stitched inversion results. The layering is less confined when compared to the 1D stitched inversion, as may be expected since we have increased the number of degrees of freedom in our inversion model. Comparisons of the observed and predicted data for the 1D and 2D inversions are shown in Figure 7. Although both predicted data from the 1D and 2D inversion results show reasonable fit with the observed data, we note some discrepancies that are likely due to 3D model complexities that are not possible to explain with a lower dimension model.

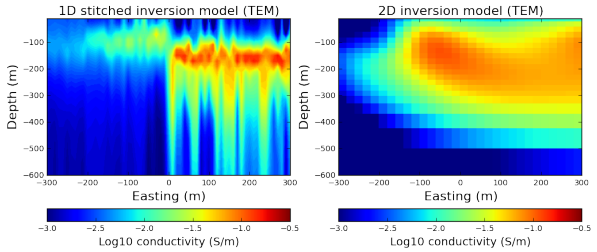

Figure 6: Vertical sections of recovered conductivity. Left and right panel show 1D stitched and 2D conductivity models recovered from 1D and 2D EM inversions, respectively.

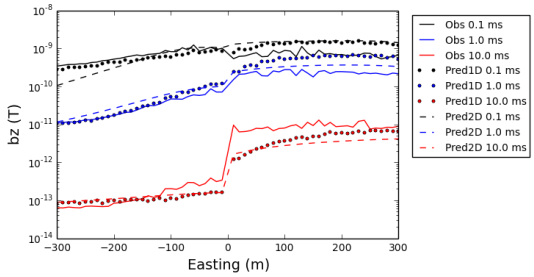

Figure 7: Comparisons of observed and predicted data for 1D and 2D inversions.

3D inversion

In reality, the distribution of intruded seawater is in 3D, thus restoration of the 3D conductivity model is an important task in order to characterize the regions that are affected by seawater intrusion. For the previous 1D and 2D inversions, we used a subset of the total data. However, for a 3D inversion, it is crucial to have measurements that are not solely collected in the center line of the loop to have reasonable sensitivity to the 3D volume. We used all receivers shown in Figure 5. Using the mapping function shown in equation 5, we perform a 3D EM inversion. Figure 8 shows plan and section views of the recovered conductivity model from the 3D inversion. The interface of the seawater intrusion is nicely imaged in both horizontal and vertical directions. A visualization of the 3D recovered volume of conductivity distribution is shown in Figure 9.

CONCLUSIONS

By using the presented mapping methodology in our geophysical inversion, we separate the inversion model space from the physical property space. This allows us flexibility in selecting a definition of an inversion model. The mapping serves

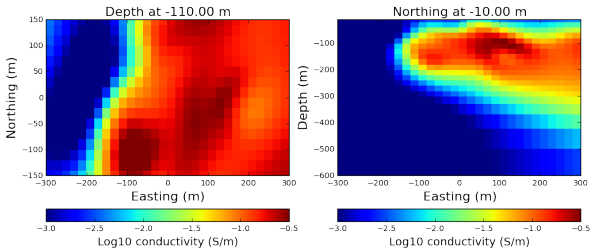

Figure 8: Plan and section views of recovered conductivity from 3D EM inversion.

as a link between the two spaces. Our inversion model may be defined in one, two, or three dimensions, and through the mapping, the 3D physical property distribution associated with this model is constructed. Data can then be simulated over this physical property distribution, and the model agreement with the observed data evaluated.

We demonstrated this concept for three different inversion models with different dimensionalities: 1D, 2D, and 3D. Using a mapping, we performed TDEM inversions for an example seawater intrusion problem. We focused our discussion on considering model spaces having differing dimensionalities, which is a small subset of the possible parameterizations available. Another option is to consider parametric mapping functions in which we seek to find a geometric shape or boundary with a small number of model parameters. These parameterizations will allow targeted questions to be asked of the inversion using the mapping methodology described here *without* changing the EM simulation and inversion 'machinery'. This separation of the inversion model space from the physical property space is a powerful concept, as it allows us to tailor our choice of model space to the geologic setting, survey design and goals of the inversion.

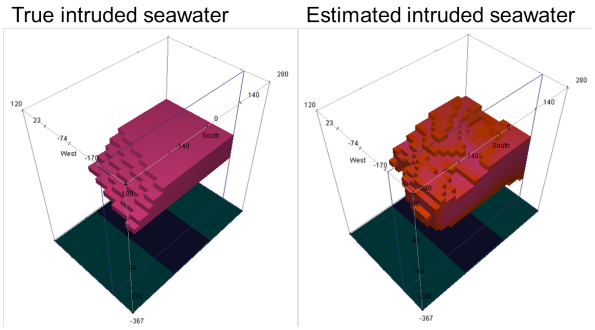

Figure 9: Cut-off 3D volume of true and recovered conductivity distribution of seawater intrusion.

ACKNOWLEDGEMENT

Thanks to Klara Steklova for helpful discussion about hydrological problem, Eldad Haber for discussions on computational electromagnetics, and SIMPEG developers. Generating the 3D seawater intrusion model was performed using GIFtools.

REFERENCES

Chung, Y., J.-S. Son, T. J. Lee, H. J. Kim, and C. Shin, 2014, Three-dimensional modelling of controlled-source electromagnetic surveys using an edge finite-element method with a direct solver: Geophysical Prospecting, **62**, 1468–1483.

Cockett, R., S. Kang, A. Heagy L., Pidlisecky, and D. Oldenburg, 2015, SimPEG: An open-source framework for simulation and parameter estimation in geophysical applications (submitted): Computers and Geoscience.

Gribenko, A., and M. Zhdanov, 2007, Rigorous 3D inversion of marine CSEM data based on the integral equation method: Geophysics, **72**, WA73–WA84.

Heagy, L. J., A. R. Cockett, and D. W. Oldenburg, 2014, 165, *in* Parametrized inversion framework for proppant volume in a hydraulically fractured reservoir: 865–869.

Kang, S., R. Cockett, and L. J. Heagy, 2015, simpegEM online documentation available at http://simpegem.rtfd.org.

McMillan, M. S., C. Schwarzbach, D. W. Oldenburg, E. Haber, E. Holtham, and A. Prikhodko, 2014, 329, *in* Recovering a thin dipping conductor with 3D electromagnetic inversion over the Caber deposit: 1720–1724.

Mills, T., P. Hoekstra, M. Blohm, and L. Evans, 1988, Time Domain Electromagnetic Soundings for Mapping SeaWater Intrusion in Monterey County, California: Ground Water.

Oldenburg, D. W., E. Haber, and R. Shekhtman, 2013, Three dimensional inversion of multisource time domain electromagnetic data: GEOPHYSICS, **78**, E47–E57.

Oldenburg, D. W., and Y. Li, 2005, 5. Inversion for Applied Geophysics: A Tutorial, *in* Near-Surface Geophysics: 5, 89–150.

Pidlisecky, A., K. Singha, and F. D. Day-Lewis, 2011, A distribution-based parametrization for improved tomographic imaging of solute plumes: Geophysical Journal International, **187**, 214–224.